FULL PAPER

Dalton
www.rsc.org/dalton

Selective oxygenation of amphiphilic thiacalix[3]pyridine Rh(I) diene complexes in both water and organic solvents

Takanori Nishioka,* Yusuke Onishi, Kunio Nakajo, Jin Guo-Xin, Rika Tanaka and Isamu Kinoshita*

Department of Material Science, Graduate School of Science, Osaka City University, Sugimoto, Sumiyoshi-ku, Osaka, 558-8585, Japan. E-mail: nishioka@sci.osaka-cu.ac.jp; Fax: 81-6-6690-2753; Tel: 81-6-6605-2569

Received 17th March 2005, Accepted 27th April 2005
First published as an Advance Article on the web 11th May 2005

Thiacalix[3]pyridine (Py_3S_3) reacted with [Rh(diene)(μ-Cl)]$_2$ (diene = 1,5-cyclooctadiene (cod), 2,5-norbornadiene (nbd)) to give amphiphilic trigonal bipyramidal complexes, [Rh(Py_3S_3)(diene)]Cl. Sulfur bridges of the Py_3S_3 ligand in these complexes were selectively oxygenated by *m*-chloroperoxybenzoic acid in dichloromethane to give sulfinylcalix[3]pyridine complexes, [Rh{$Py_3(SO)_3$}(diene)]$^+$, in which all three oxygen atoms of the SO groups occupy the equatorial positions. Structures of the complexes were analysed by X-ray crystallography and the oxidation reaction was investigated using ^{1}H NMR spectroscopy and electrospray ionisation mass spectrometry showing that the oxygenation of the sulfur atoms in the ligand proceeded stepwise and further oxygenation of the SO moiety occurred only for the nbd complex having the smaller diene ligand resulting in [Rh{$Py_3(SO)_2(SO_2)$}(nbd)]$^+$. On the other hand, the oxidation of [Rh(Py_3S_3)(cod)]$^+$ by H_2O_2 in water did not result in oxygenation of the sulfur bridges but the cod ligand is hydroxygenated to give 1,4,5,6-η^4-2-hydroxycycloocta-4-ene-1,6-di-yl.

Introduction

Macrocyclic polypyridines are potentially powerful ligands which can promote significant functionalities such as C–H bond activation by the platinum complex of pyridinophane.[1] However, only limited examples of macrocyclic polypyridine complexes have been reported.[2] We have prepared the first example of a transition metal complex of a macrocyclic polypyridine ligand with threefold rotational symmetry, bis(thiacalix[3]pyridine)dicopper(I), [Cu(Py_3S_3)]$_2^{2+}$, which has a dimeric structure through the compensatory coordination of one of the sulfur atoms in the ligand to another copper ion.[3] Another facial coordinating N tridentate ligand, triazacyclononane (tacn) can stabilise higher oxidation states such as Ni^{III}.[4] This property of the tacn ligand also stabilised an intermediate with a higher oxidation state of the metal centre in the case of the selective oxidation of [Rh(Me_3tacn)(cod)]$^+$ (Me_3tacn = 1,4,7-trimethyl-1,4,7-triazacyclononane) by H_2O_2. In this system, the rhodium(I) cod complex was oxidised by H_2O_2 to afford the rhodium(III) oxabicyclononadiyl complex which rearranged to the rhodium(III) hydroxycyclooctenediyl complex. A rhodaoxetane was suggested to be the key intermediate of these oxygenation reactions.[5] For the [Rh(Py_3S_3)(diene)]$^+$ complexes, there are some possible sites for oxygenation, for example, the diene ligand (the same as in the Me_3tacn system) and the bridging sulfur of the Py_3S_3 ligand. In this paper, we describe the oxidation reaction of newly synthesised amphiphilic thiacalix[3]pyridine Rh complexes, [Rh(Py_3S_3)(diene)]Cl (diene = 1,5-cyclooctadiene (cod), 2,5-norbornadiene (nbd)) using H_2O_2 in water or *m*-chloroperoxybenzoic acid (*m*-CPBA) in CH_2Cl_2.

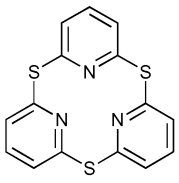

Thiacalix[3]pyridine (Py_3S_3)

Results and discussion

Formation of complexes

[Rh(Py_3S_3)(cod)]Cl (**1a**) was synthesised by the reaction of [Rh(cod)(μ-Cl)]$_2$ and Py_3S_3 in methanol with a 1 : 2 molar ratio of the starting materials.

$$[Rh(diene)(\mu\text{-}Cl)]_2 + 2\ Py_3S_3 \rightarrow 2[Rh(Py_3S_3)(diene)]Cl$$

The ^{1}H NMR spectrum of an *in situ* reaction mixture revealed only the signals corresponding to one Py_3S_3 and one cod ligand and the electrospray ionisation (ESI) mass spectrum showed only the complex cation peak at $m/z = 538$. These results show that the reaction proceeded quantitatively. The BPh_4 salt (**1b**) was easily isolated by the addition of $NaBPh_4$ to the reaction mixture owing to the low solubility of the salt in methanol. [Rh(Py_3S_3)(nbd)]X (X = Cl, **2a**; BPh_4, **2b**) was also synthesised in a similar manner. Complexes **1a** and **2a** were soluble in both water and organic solvents such as CH_2Cl_2. X-Ray diffraction studies were performed for the BPh_4 salts **1b** and **2b** and the structures of the cationic complexes are shown in Fig. 1.

Oxidation of [Rh(Py_3S_3)(cod)]$^+$ and [Rh(Py_3S_3)(nbd)]$^+$

The cod complex **1** was oxidised by *m*-chloroperoxybenzoic acid (*m*-CPBA) in CH_2Cl_2 for 24 h to give a sulfinylcalix[3]pyridine complex [Rh{$Py_3(SO)_3$}(cod)]$^+$ in high yield.

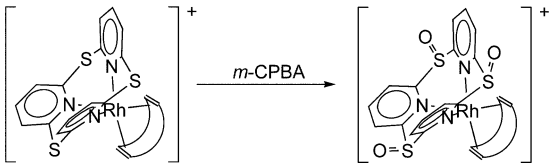

X-Ray structure analysis of the BPh_4 salt (**3b**) revealed that all three oxygen atoms of the SO groups in the complex occupy equatorial positions as shown in Fig. 2. The Py_3S_3 ligand in **1** adopts the cone shape conformation and the oxygenation occurred on the opposite side to the {Rh(cod)} unit. The ESI mass spectrum of the reaction mixture of **1** and 10 eq. of *m*-CPBA after 3.5 h, Fig. 3(b), showed a dominant peak at m/z = 554 for [Rh(Py_3S_3O)(cod)]$^+$ beside the much smaller peaks of **1**

DOI: 10.1039/b503924j

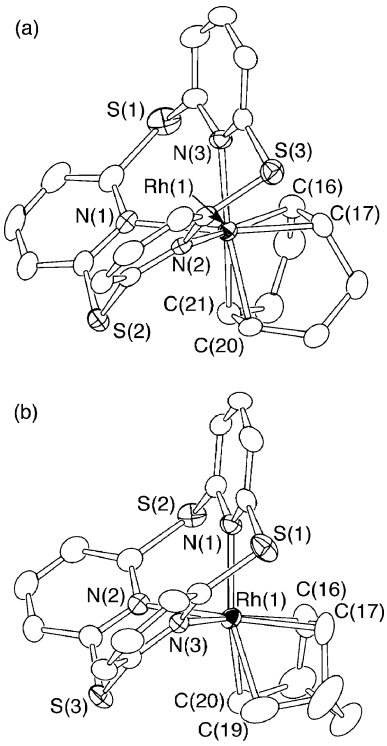

Fig. 1 ORTEP drawing of the cationic moieties of (a) [Rh(Py_3S_3)(cod)](BPh_4) **1b** and (b) [Rh(Py_3S_3)(nbd)](BPh_4) **2b**. All hydrogen atoms have been deleted for clarity.

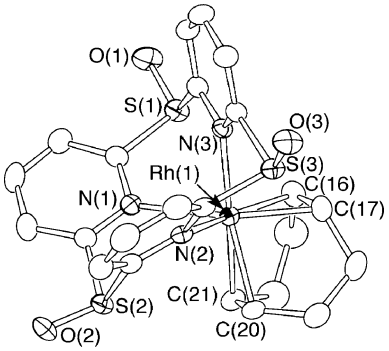

Fig. 2 ORTEP drawing of the cationic moiety of [Rh{$Py_3(SO)_3$}(cod)](BPh_4) **3b**. All hydrogen atoms have been deleted for clarity.

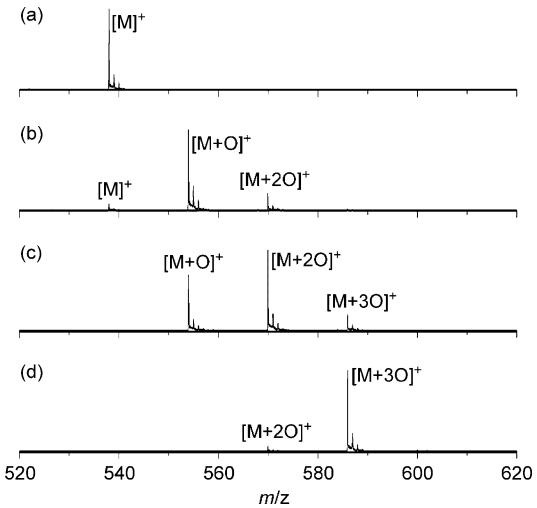

Fig. 3 ESI mass spectra of (a) **1b** and the reaction mixture of complex **1b** and 10 eq. of *m*-CPBA after (b) 3.5 h, (c) 6.5 h and (d) 24 h.

and [Rh($Py_3S_3O_2$)(cod)]$^+$ at m/z = 538, 570, respectively. This result suggests that the oxygenation of **1** proceeds stepwise. No peaks corresponding to the complex having more than four oxygen atoms were observed after generation of the trioxygenated complex **3** shown in Fig. 3(d) meaning that the oxygenation stopped at this stage. In contrast to the oxidation of the complex, the oxidation of the free Py_3S_3 ligand by 10 eq. of *m*-CPBA for 24 h gave a mixture of $Py_3S_3O_3$, $Py_3S_3O_4$, $Py_3S_3O_5$ and $Py_3S_3O_6$ confirmed by the ESI mass spectrum showing peaks at m/z = 398, 414, 430 and 446 ([M + Na]$^+$) with 48%, 100%, 21% and 5% relative intensities, respectively, Fig. 4(b). The result apparently indicates that the oxidation of the free ligand produced not only sulfinyl but also sulfonyl. In the case of the oxidation of **1**, molecules of *m*-CPBA could approach the Py_3S_3 ligand in the complex only from the less hindered side of the ligand with the help of the π–π interaction between the benzene ring of *m*-CPBA and the pyridine rings of the ligand. It means that the selectivity of the oxygenation reaction is attributed to the steric hindrance of the cod ligand. Similar oxygenation of sulfur bridges was reported for thiacalix[4]arenes.[6] The oxidation of *p-tert*-butylthiacalix[4]arene afforded several stereoisomers of *p-tert*-butylsulfinylcalix[4]arene due to the existence of conformers and unselective oxygenation. Separation of each conformer before oxidation became possible by introducing the bulky *O*-benzylester groups and oxygenation occurred on the other side of the *O*-benzylester groups, for example, the oxidation of its separated cone conformer by $NaBO_3$ gave only one stereoisomer due to steric hindrance.[6] In the case of oxidation of **1**, coordination of the Py_3S_3 ligand to the {Rh(cod)} unit has an important role in limiting the approach direction of the oxidising agent and in fixing the cone conformation of the Py_3S_3 ligand, which adopts an alternate conformation as a free ligand.[7]

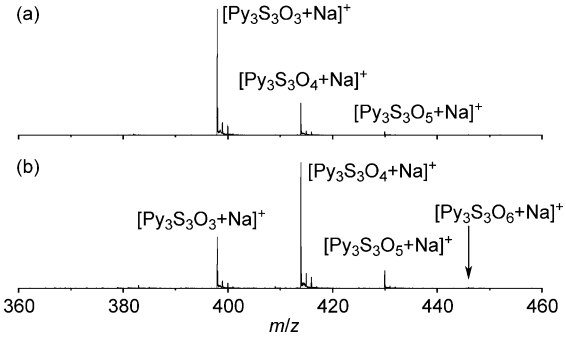

Fig. 4 ESI mass spectra of the reaction mixture of Py_3S_3 and 10 eq. of *m*-CPBA after (a) 1 h and (b) 24 h.

Mono- and di-oxygenated complexes were also observed in the ^{1}H NMR spectrum during the reaction of **1** with *m*-CPBA. The ^{1}H NMR spectrum of the oxygenated complexes showed complicated patterns in the pyridine region and downfield-shifted cod signals, Fig. 5(b). The complicated signals were observed in the pyridine region and they are attributed to the overlap of two sets of AB_2 and ABB′ signals of the oxygenated Py_3S_3 ligands. The signal patterns of the cod ligands were unchanged after oxidation. These results mean that the cod

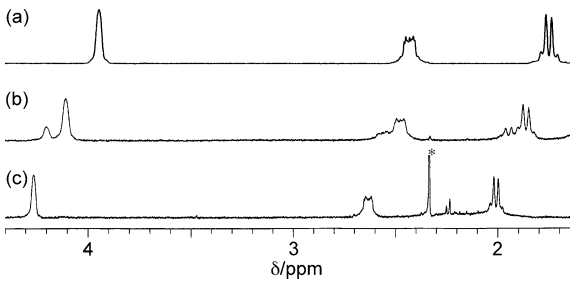

Fig. 5 The cod ligand region of the ^{1}H NMR spectra in $CDCl_3$ of (a) complex **1**, (b) the oxidation product of **1** by *m*-CPBA for 2 h and (c) complex **3**. The peak marked with * is the signal of the CH_3 group of toluene used for crystallisation.

ligand was not oxygenated but that the Py_3S_3 ligand was oxidised to give S-oxygenated Py_3S_3 complexes, $[Rh(Py_3S_3O)(cod)]^+$ and $[Rh(Py_3S_3O_2)(cod)]^+$ consistent with the result of the ESI-MS. Because the structure of the final product was confirmed as $[Rh\{Py_3(SO)_3\}(cod)]^+$, the dioxygenated complex does not contain SO_2 groups and these mono- and di-oxygenated complexes should be $[Rh\{Py_3S_2(SO)\}(cod)]^+$ and $[Rh\{Py_3S(SO)_2\}(cod)]^+$, respectively. A set of ^1H NMR signals for the cod ligand in the dioxygenated Py_3S_3 complex appeared at lower field than that in the monooxygenated one. It means less electron density on the cod ligand in the dioxygenated complex, and oxidation of the Py_3S_3 ligand withdraws electrons from the Rh centre. Because the oxygen atoms in **3b** sit on the equatorial positions, the oxygen atoms in the mono- and di-oxygenated complexes should occupy the equatorial positions.

The norbornadiene complex **2** was also oxidised by *m*-CPBA resulting in the S oxygenated complexes. However, ESI-MS showed that the oxygenation proceeded until four oxygen atoms were added to the complex, Fig 6. The mono- and di-oxygenated complexes were crystallised as mixed-crystals by addition of $NaBPh_4$ to a methanol solution of the mixture of these complexes. X-Ray analysis of the mixed-crystal revealed that the O(2) atom had less than 1.0 occupancy meaning that the crystal contained both mono- and di-oxygenated complexes, $[Rh\{Py_3S_2(SO)\}(nbd)]^+$ (**4**) and $[Rh\{Py_3S(SO)_2\}(nbd)]^+$ (**5**), and only the S atoms of the Py_3S_3 ligands were oxygenated, Fig. 7(a). The result of ESI-MS of the crystal also supported the fact that it was a mixed-crystal, Fig. 7(b). ^1H NMR spectra of a mixture of tri- and tetra-oxygenated complexes (Fig. 8(b)) showed the signal pattern of the nbd ligand to be unchanged after oxygenation implying that third and forth oxygenation also occurred at the sulfur bridges, but not at the nbd ligands, to give $[Rh\{Py_3(SO)_3\}(nbd)]^+$ (**6**) and $[Rh\{Py_3(SO)_2(SO_2)\}(nbd)]^+$ (**7**), respectively. Since the nbd ligand consists of a six-membered ring (if the bridge-head CH_2 is not taken into account) and is smaller than the cod ligand which has an eight-membered ring. As a result, steric hindrance at the Rh-diene side of the Py_3S_3 ligand in the nbd complex is less than that in the cod complex causing the fourth oxygenation reaction. Isolation of pure **7** has not been successful because of the instability of **7** in the presence of *m*-CPBA or *m*-chlorobenzoic acid and comparably slow reaction rate.

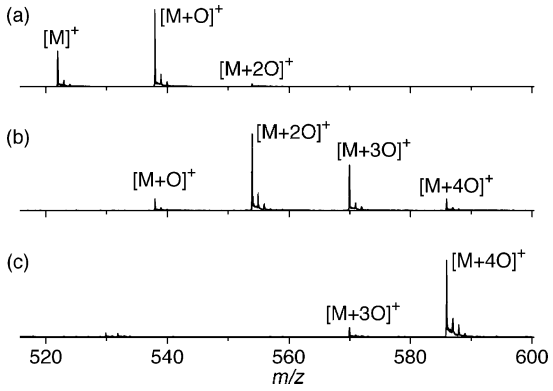

Fig. 6 ESI mass spectra of the reaction mixture of complex **2b** and 10 eq. of *m*-CPBA after (a) 2 h, (b) 7 h, (c) 8 h and additional 2 h after further addition of 20 eq. of *m*-CPBA.

Although oxygenation occurred only at the sulfur bridges of Py_3S_3 using *m*-CPBA, oxidation by H_2O_2 afforded the monooxygenated complex, **8b**, in which the cod ligand was hydroxygenated. ESI mass spectrum of the reaction mixture of **1a** and H_2O_2 in H_2O dominantly revealed the peaks of the monooxygenated complex, Fig. 9. The ^1H NMR spectrum of the product obtained by addition of $NaBPh_4$ to the reaction mixture showed a complicated pattern over 1–6 ppm beside the signals for the unoxygenated starting material **1**, Fig. 10. X-Ray analysis

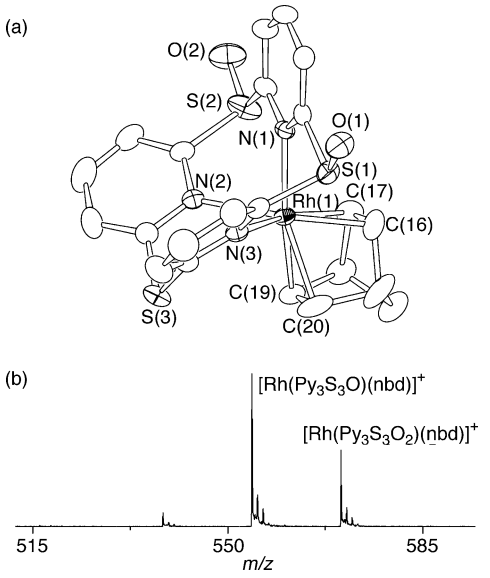

Fig. 7 (a) ORTEP drawing of the cationic moiety of the oxygenated nbd complex. All hydrogen atoms have been deleted for clarity. The disorder of the O(2) atom suggested that the crystal contained both di- and mono-oxygenated complexes. (b) ESI-MS of the crystal used for X-ray analysis clearly showed the signals for both mono- and di-oxygenated complexes.

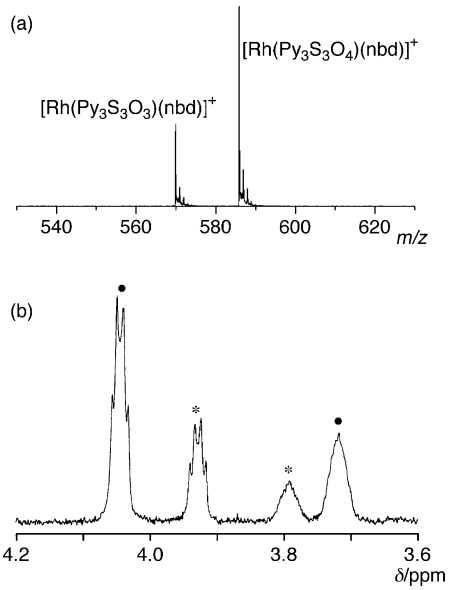

Fig. 8 (a) ESI mass and (b) ^1H NMR spectra of the mixture of $[Rh(Py_3S_3O_3)(nbd)](BPh_4)$ **6b** (*) and $[Rh(Py_3S_3O_4)(nbd)](BPh_4)$ **7b** (●).

of **8b** shown in Fig. 11 clearly showed that the sulfur bridges remained unoxygenated and the cod ligand was hydroxygenated to 1,4,5,6-η^4-2-hydroxycycloocta-4-ene-1,6-di-yl, so the peak at $m/z = 554$ in the ESI mass spectrum was assigned to the complex with a hydroxygenated cod ligand whose structure has eleven inequivalent protons and is consistent with the ^1H NMR spectrum in Fig. 10. The same hydroxygenation of the cod ligand was reported for the oxidation of rhodium and iridium cod complexes.[5b,8] These Rh cod complexes were oxidised by H_2O_2 to afford oxabicyclononadiyl complexes which were converted to hydroxycyclooctenediyl ones by heating at 80 °C. In the Py_3S_3 system, only the hydroxycyclooctenediyl complex was isolated in the oxidation by H_2O_2 at room temperature. Additionally, no oxidation reaction occurred when the same reaction time (1 h) as the Me_3tacn complexes was applied.

In the ESI mass spectrum of the reaction mixture of H_2O_2 oxidation (Fig. 9(b)), a small signal for the dioxygenated complex was observed. It is unclear whether the sulfur bridge

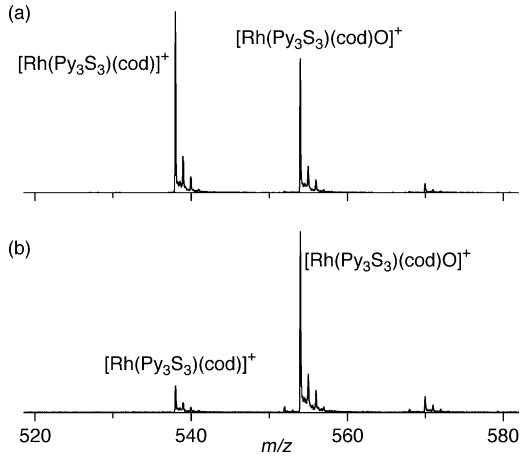

Fig. 9 ESI mass spectra of the reaction mixture of $[Rh(Py_3S_3)(cod)]^+$ and H_2O_2 after (a) 4 h and (b) 24 h.

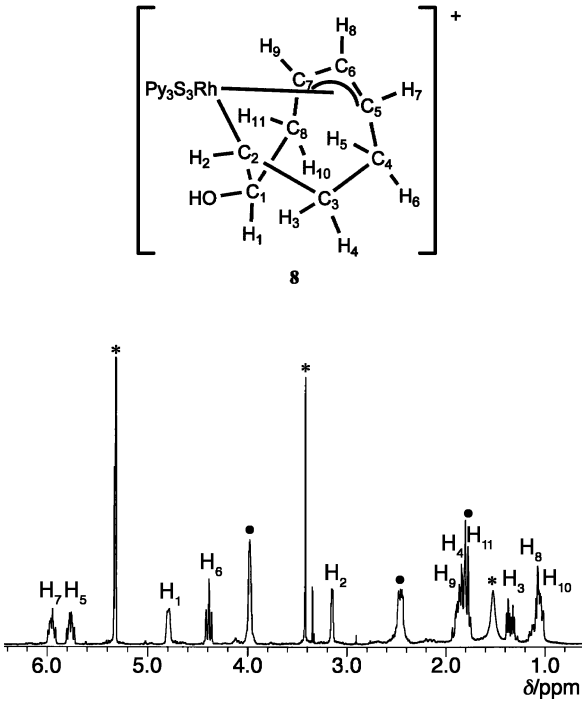

8

Fig. 10 ^1H NMR spectrum (400 MHz, cod region) of the mixture of $[Rh(Py_3S_3)(cod)]^+$ (●) and the H_2O_2 oxygenated complex **8**. The signals marked with * are of solvents.

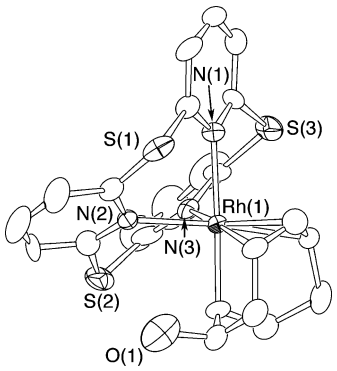

Fig. 11 ORTEP drawing of the cationic moiety of **8b**. Although X-ray crystallography showed two independent cations of the complex in the asymmetric unit, one of them is shown because they have almost the same structures.

or the carbon atom in the cod moiety was oxygenated and the second oxygenation seems to be slower. In the case of oxidation by H_2O_2, oxygenation of the sulfur bridges did not proceed or was very slow if it occurred. This is probably attributed to the lack of π–π interactions with the pyridine ring of the Py_3S_3 ligand supposed for *m*-CPBA oxidation. Oxygenation of rhodium and iridium complexes with N_3 ligands afforded the cod ligands oxygenated *via* oxygen-coordinated intermediates.[5] In the case of the oxygenation of **1** by H_2O_2, a similar intermediate containing Rh^{III}–O could be concerned. On the other hand, such intermediates were not involved in *m*-CPBA oxygenation.

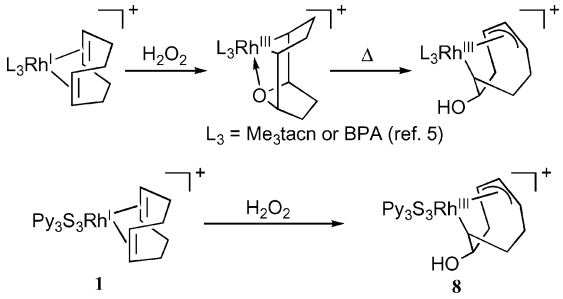

1 **8**

Structures of the complexes

X-Ray crystal structure analyses were performed for **1b, 2b, 3b, 6b** (see Fig. 12), **8b** and the mixed crystal **4b/5b**, but **8b** is excluded from the structural discussion because of the poor quality of the data due to the poor quality of the crystal used for the analysis. Selected bond lengths and angles are listed in Table 1. The coordination geometry around the Rh atom in **1b** is trigonal bipyramidal similar to the 1,4,7-trimethyl-1,4,7-triazacyclononane (Me_3tacn) analogue.[6] In complex **1b**, the axial Rh–C(olefin) bond lengths (av. 2.167(4) Å) are longer than the equatorial ones (av. 2.081(5) Å) and these values and trends were the same as those found in the Me_3tacn complex (av. 2.164(6) Å for axial, av. 2.080(4) Å for equatorial). While the arrangement of the cod ligands around the Rh atoms in **1b** and the Me_3tacn complex are almost the same, the Rh–N distances (Rh–N_{ax}, 2.092(3) Å; Rh–N_{eq}, 2.293(3) and 2.314(3) Å) and N–Rh–N angles (N_{ax}–Rh–N_{eq}, 84.9(1) and 83.2(1)°; N_{eq}–Rh–N_{eq}, 79.7(1)°) in **1b** were shorter and wider than those found in the Me_3tacn complex (Rh–N_{ax}, 2.198(2) Å; Rh–N_{eq}, 2.339(2) and 2.335(2) Å; N_{ax}–Rh–N_{eq}, 80.09(9) and 78.91(9)°; N_{eq}–Rh–N_{eq}, 76.77(9)°).

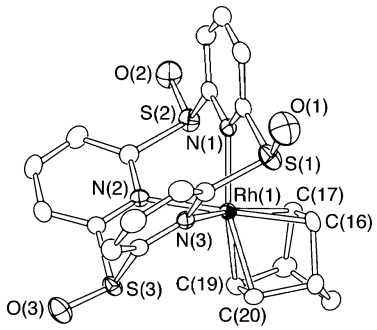

Fig. 12 ORTEP drawing of the cationic moiety of $[Rh\{Py_3(SO)_3\}(nbd)](BPh_4)$ **6b**. All hydrogen atoms have been deleted for clarity.

The coordination geometry around the Rh atom in each unoxygenated complex, **1b** or **2b**, is very similar to the corresponding trioxygenated complex, **3b** or **6b**, and the Rh–N distances and the N–Rh–N angles are almost the same. Between the structures of the unoxygenated and corresponding trioxygenated complexes, significant differences appear around the bridging sulfur atoms. The S–C bond lengths are in the range 1.764(4)–1.777(4) Å in **1b** and **2b** and become longer after oxidation (1.808(3)–1.822(2) Å in **3b** and **6b**). The C–S–C angles in the unoxygenated complexes (98.9(2), 102.8(2) and 104.3(2)° in **1b**, 101.3(1), 101.4(1) and 102.4(1)° in **2b**) become smaller after oxidation (91.4(1), 93.6(1) and 94.4(1)° for **3b**, 94.0(1), 94.1(1) and 95.4(1)° for **6b**). Similar structural

Table 1 Selected bond lengths (Å) and angles (°) in **1b, 2b, 3b, 6b** and the mixed crystal **4b/5b**

	1b	2b	3b	4b/5b	6b
Rh–N_{ax}	2.092(3)	2.120(2)	2.078(2)	2.069(3)	2.086(2)
Rh–N_{eq}	2.293(3), 2.314(3)	2.233(2), 2.242(2)	2.294(2), 2.326(2)	2.232(2), 2.262(3)	2.265(2), 2.271(2)
Rh–C_{ax}	2.164(4), 2.170(4)	2.138(3), 2.149(4)	2.188(2), 2.208(2)	2.167(4), 2.170(4)	2.172(3), 2.187(3)
Rh–C_{eq}	2.076(4), 2.085(4)	2.075(3), 2.086(3)	2.092(3), 2.100(3)	2.062(5), 2.066(4)	2.080(3), 2.085(3)
Rh–Ctr(C=C)$_{ax}$[a]	2.055(4)	2.035(4)	2.088(2)	2.059(4)	2.070(3)
Rh–Ctr(C=C)$_{eq}$[a]	1.954(4)	1.961(3)	1.970(3)	1.940(4)	1.958(3)
C–S	1.764(4), 1.770(4)	1.771(3), 1.772(3)	1.811(3), 1.811(3)	1.776(4), 1.778(4)	1.808(3), 1.813(3)
	1.774(4), 1.774(4)	1.774(3), 1.775(3)	1.811(3), 1.814(3)	1.791(4), 1.806(4)	1.814(3), 1.814(3)
	1.776(4), 1.777(4)	1.776(3), 1.777(3)	1.821(2), 1.822(2)	1.807(4), 1.809(4)	1.816(3), 1.817(3)
S–O			1.478(2), 1.485(2)	1.419(4), 1.483(3)	1.456(2), 1.478(2)
			1.487(2)		1.481(2)
C=C_{ax}	1.375(6)	1.350(6)	1.372(4)	1.357(7)	1.366(4)
C=C_{eq}	1.426(6)	1.394(5)	1.429(4)	1.408(7)	1.417(4)
N_{ax}–Rh–N_{eq}	83.2(1), 84.9(1)	85.02(8), 85.31(8)	83.72(7), 84.20(7)	85.6(1), 85.64(9)	85.24(8), 85.35(8)
N_{eq}–Rh–N_{eq}	79.7(1)	82.08(8)	78.34(7)	81.1(1)	80.55(8)
N_{ax}–Rh–Ctr(C=C)$_{ax}$[a]	176.1(1)	167.6(1)	175.60(9)	167.4(2)	167.5(1)
N_{ax}–Rh–Ctr(C=C)$_{eq}$[a]	90.1(2)	96.7(1)	91.09(10)	97.5(1)	97.24(10)
N_{eq}–Rh–Ctr(C=C)$_{ax}$[a]	97.8(1), 100.0(1)	103.2(1), 104.8(1)	96.12(9), 100.65(9)	102.1(1), 105.3(2)	103.92(9), 104.37(10)
N_{eq}–Rh–Ctr(C=C)$_{eq}$[a]	137.3(2), 141.8(2)	138.4(1), 139.6(1)	137.04(10), 143.67(10)	136.4(2), 142.4(2)	137.62(10), 141.81(10)
C–S–C	98.9(2), 102.8(2)	101.3(1), 101.4(1)	91.4(1), 93.6(1)	95.7(2), 98.0(1)	94.0(1), 94.3(1)
	104.3(2)	102.4(1)	94.4(1)	99.9(2)	95.4(1)
C–S–O			104.8(1), 105.6(1)	105.5(2), 105.8(1)	105.8(1), 106.6(1)
			105.7(1), 106.2(1)	108.3(2), 111.3(2)	107.1(1), 107.7(1)
			106.5(1), 106.9(1)		107.9(1), 108.6(1)

[a] Ctr(C=C): Central position between olefin carbon atoms.

changes upon oxygenation of the bridging S atoms were observed in *p-tert*-butylthiacalix[4]arene tetra-*O*-benzylester (S–C, 1.781(4)–1.785(4) Å; C–S–C, 99.4(2) and 99.7(2)°) and *p-tert*-butylsulfinylcalix[4]arene tetra-*O*-benzylester (S–C, 1.810(5) and 1.814(5) Å; C–S–C, 97.4(2)°).[6] Although the C–S–C values in **1b** vary widely, the distribution of those found in **3b** is much smaller. The large distribution of the C–S–C angles in **1b** is probably attributed to steric repulsion caused by the cod ligand around the metal ion. On the other hand, the distributions of the C–S–C values of both **2b** and **6b** are smaller than those of the cod complexes. The flexible C–S–C bonds in the Py_3S_3 ligand allows changes in its conformation to reduce the steric hindrance in **1b**. These structural features probably affect the reactivity upon the fourth oxygenation of the sulfur bridges which occurs only for the less hindered nbd complex.

Conclusions

We have synthesised the amphiphilic thiacalix[3]pyridine rhodium cod and nbd complexes and have demonstrated their selective oxidation by *m*-CPBA to give the sulfinylcalix[3]pyridine rhodium complexes. The selectivity of the oxygenation is attributed to steric hindrance of the diene ligands and to the fixed conformation of the ligand by coordination to a Rh ion. Oxidation of the cod complex by H_2O_2 did not result in oxygenation of the sulfur bridges in the Py_3S_3 ligand but hydroxygenation of the cod ligand to give a 1,4,5,6-η^4-2-hydroxycycloocta-4-ene-1,6-diyl rhodium(III) complex. The reactions reported in this paper are summarised in Scheme 1.

Experimental

Materials

All solvents were purchased from Nacalai Tesque for the reactions and from Sigma-Aldrich Japan or Merck for the measurements and used without further purification. Thiacalix[3]pyridine was synthesised by the literature procedure.[3a] *m*-Chloroperoxybenzoic acid was purified by washing with phosphate buffer (1/15 mol l^{-1}, pH 7.0). All other reagents were used as received.

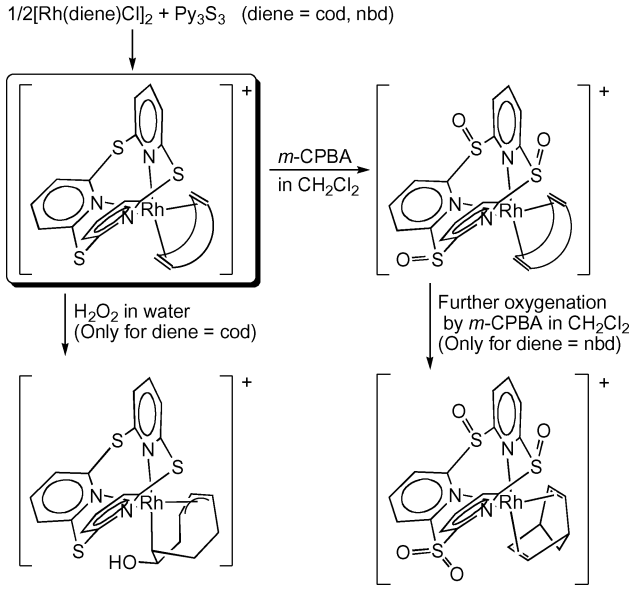

Scheme 1

General procedures

^{1}H and ^{13}C NMR spectra were recorded on JEOL Lambda300 and 400 and Bruker AVANCE600 FT-NMR spectrometers, and chemical shifts were referenced to tetramethylsilane. Electrospray ionisation (ESI) mass spectrometry measurements were performed on an Applied Biosystem Mariner spectrometer using HPLC grade solvents. Elemental analyses were performed by the Analytical Research Service Centre at Osaka City University on Perkin Elmer 240C or FISONS Instrument EA108 elemental analysers.

Synthesis of [Rh(Py_3S_3)(diene)]$^+$ (diene = cod, nbd) complexes

Synthesis of [Rh(Py_3S_3)(cod)]Cl (1a). Thiacalix[3]pyridine (Py_3S_3, 327 mg, 1.00 mmol) and [Rh(cod)(μ-Cl)]$_2$ (247 mg, 0.50 mmol) were stirred in 20 ml of methanol for 10 min

resulting in a yellow orange solution. After a small amount insoluble solid was filtered off, the solvent of the filtrate was removed under reduced pressure to give a yellow solid of [Rh(Py_3S_3)(cod)]Cl (**1a**) (546 mg, 95%). The crude product was recrystallised from an aqueous solution by slow evaporation of the solvent to afford orange crystals of the hydrated complex, [Rh(Py_3S_3)(cod)]Cl·2.5H_2O (Found: C, 44.79; H, 4.07; N, 6.73. $C_{23}H_{26}N_3O_{2.5}RhS_3$ requires C, 44.63; H, 4.23; N, 6.79%); δ_H(300 MHz, CD_3OD, TMS) 7.94 (9H, AB_2 multiplet, pyridyl), 4.03 (4H, br, –C*H*=), 2.47 (4H, m, *exo* –CH_2–), 1.80 (4H, m, *endo* –CH_2–); ESI-MS m/z = 538 ([M − Cl]$^+$).

Synthesis of [Rh(Py_3S_3)(cod)](BPh_4) (1b). A solution of Py_3S_3 (327 mg, 1.00 mmol) in 60 mL of methanol was added to a suspension of [Rh(cod)(μ-Cl)]$_2$ (247 mg, 0.50 mmol) in 40 ml of methanol and the mixture was stirred for 2 h to give a yellow orange solution. Slow addition of a solution of $NaBPh_4$ (420 mg, 1.23 mmol) in methanol (20 ml) afforded a yellow microcrystalline solid of [Rh(Py_3S_3)(cod)](BPh_4) (**1b**). After further stirring for 1 h, the solid was collected by filtration and washed with methanol and diethyl ether (853 mg, 99%) (Found: C, 65.71; H, 4.74; N, 4.85. $C_{47}H_{41}BN_3RhS_3$ requires C, 65.81, H, 4.82; N, 4.90%); δ_H(600 MHz, $CDCl_3$, TMS) 7.60 (6H, d, $^3J_{H-H}$ = 7.8 Hz, 3,5-pyridyl), 7.49 (3H, t, $^3J_{H-H}$ = 7.8 Hz, 4-pyridyl), 7.32 (8H, m, *o*-phenyl), 6.82 (8H, t, $^3J_{H-H}$ = 7.2 Hz, *m*-phenyl), 6.68 (4H, t, $^3J_{H-H}$ = 7.2 Hz, *p*-phenyl), 3.82 (4H, br, –C*H*=), 2.35 (4H, m, *exo* –CH_2–), 1.68 (4H, m, *endo* –CH_2–); δ_C(150 MHz, $CDCl_3$, TMS) 166.5 (m, *i*-phenyl), 155.7 (s, 2,6-pyridyl), 141.3 (s, 4-pyridyl), 136.2 (s, o-phenyl), 128.9 (s, 3,5-pyridyl), 125.4 (s, *m*-phenyl), 121.6 (s, *p*-phenyl), 76.5 (br, –*C*H=), 30.7 (s, –*C*H_2–); ESI-MS m/z = 538 ([M − BPh_4]$^+$).

Synthesis of [Rh(Py_3S_3)(nbd)]Cl (2a). [Rh(Py_3S_3)(nbd)]Cl was prepared in a manner similar to that of the cod complex [Rh(Py_3S_3)(cod)]Cl (**1a**) using [Rh(nbd)(μ-Cl)]$_2$ (230 mg, 0.50 mmol) instead of [Rh(cod)(μ-Cl)]$_2$. Yield 520 mg, 93%. The crude product was recrystallised from an aqueous solution by slow evaporation of the solvent to afford orange crystals of the hydrated complex, [Rh(Py_3S_3)(nbd)]Cl·1.5H_2O (Found: C, 45.37; H, 3.40; N, 7.06. $C_{22}H_{20}N_3O_{1.5}RhS_3$ requires C, 45.17; H, 3.45; N, 7.18%); δ_H(300 MHz, CD_3OD, TMS) 7.95 (9H, AB_2 multiplet, pyridyl), 3.55 (2H, m, –C*H*–), 3.51 (4H, dd, J = 2.3 and 4.8 Hz, –C*H*=), 1.13 (2H, t, $^3J_{H-H}$ = 1.5 Hz, H-bridge-head); δ_C(75 MHz, CD_3OD, TMS) 157.3 (s, 2,6-pyridyl), 141.1 (s, 4-pyridyl), 129.9 (s, 3,5-pyridyl), 59.8 (d, J_{H-Rh} = 6.9 Hz, bridge-head), 47.7 (d, J_{H-Rh} = 2.9 Hz, –*C*H–), 41.7 (d, J_{H-Rh} = 10.4 Hz, –*C*H=); ESI-MS m/z = 522 ([M − Cl]$^+$).

Synthesis of [Rh(Py_3S_3)(nbd)](BPh_4) (2b). [Rh(Py_3S_3)-(nbd)](BPh_4) was prepared in a manner similar to that of the cod complex [Rh(Py_3S_3)(cod)](BPh_4) (**1b**) using [Rh(nbd)(μ-Cl)]$_2$ (230 mg, 0.50 mmol) instead of [Rh(cod)(μ-Cl)]$_2$. Yield 558 mg, 66% (Found: C, 64.96; H, 4.38; N, 4.72. $C_{46}H_{37}BN_3RhS_3$ requires C, 65.64, H, 4.43; N, 4.99%); δ_H(300 MHz, CD_2Cl_2, TMS) 7.64–7.75 (9H, AB_2 multiplet, pyridyl), 7.31 (8H, m, *o*-phenyl), 6.99 (8H, t, $^3J_{H-H}$ = 7.4 Hz, *m*-phenyl), 6.83 (4H, t, $^3J_{H-H}$ = 7.2 Hz, *p*-phenyl), 3.57 (2H, m, –C*H*–), 3.45 (4H, dd, J = 2.2 and 5.0 Hz, –C*H*=), 1.15 (2H, t, $^3J_{H-H}$ = 1.6 Hz, H-bridge-head); δ_C(75 MHz, CD_2Cl_2, TMS) 164.4 (m, *i*-phenyl), 156.0 (s, 2,6-pyridyl), 139.8 (s, 4-pyridyl), 136.3 (s, *o*-phenyl), 129.1 (s, 3,5-pyridyl), 125.9 (s, *m*-phenyl), 122.1 (s, *p*-phenyl), 58.2 (s, bridge-head), 47.0 (d, J_{H-Rh} = 2.9 Hz, –*C*H–), 41.2 (d, J_{H-Rh} = 9.8 Hz, –*C*H=); ESI-MS m/z = 522 ([M − BPh_4]$^+$).

Oxidation of [Rh{Py_3S_3}(diene)]$^+$ complexes

Oxidation of [Rh(Py_3S_3)(cod)]Cl by *m*-chloroperoxybenzoic acid. A solution of *m*-chloroperoxybenzoic acid (*m*-CPBA, 126 mg, 0.73 mmol) in 10 ml of CH_2Cl_2 was added to a solution of **1a** (42 mg, 0.073 mmol) in 5 ml of CH_2Cl_2. After stirring for 12 h, a solution of $NaBPh_4$ (48 mg, 0.15 mmol) in 15 mL methanol was added and the solution was concentrated to *ca.* 10 mL under reduced pressure to give a yellow precipitate of [Rh{$Py_3(SO)_3$}(cod)](BPh_4) (**3b**) which was collected by filtration (55 mg, 83%) (Found C, 62.07; H, 4.57; N, 4.54. $C_{47}H_{41}BN_3O_3RhS_3$ requires C, 62.32; H, 4.56; N, 4.64%); δ_H(600 MHz, $CDCl_3$, TMS) 8.30–8.38 (9H, AB_2 multiplet, pyridyl), 7.27 (8H, m, *o*-phenyl), 6.95 (8H, t, $^3J_{H-H}$ = 7.2 Hz, *m*-phenyl), 6.79 (4H, t, $^3J_{H-H}$ = 7.2 Hz, *p*-phenyl), 4.28 (4H, br, –C*H*=), 2.62 (4H, br, *exo* –CH_2–), 2.02 (4H, dd, $^2J_{H-H}$ = 16.4, $^2J_{H-Rh}$ = 7.9 Hz, *endo* –CH_2–); δ_C(150 MHz, $CDCl_3$, TMS) 165.2 (m, *i*-phenyl), 157.1 (s, 2,6-pyridyl), 142.1 (s, 4-pyridyl), 136.5 (s, *o*-phenyl), 126.7 (s, 3,5-pyridyl), 126.1 (s, *m*-phenyl), 122.2 (s, *p*-phenyl), 81.4 (d, $^1J_{C-Rh}$ = 12.3 Hz, –*C*H=), 30.8 (s, –*C*H_2-); ESI-MS m/z = 586 ([M − BPh_4]$^+$).

Oxidation of [Rh(Py_3S_3)(nbd)]Cl by *m*-chloroperoxybenzoic acid. Oxidation reaction of **2a** (216 mg, 0.387 mmol) by *m*-CPBA (668 mg, 3.87 mmol) in 50 ml of CH_2Cl_2 was examined in a similar manner to that of **1a** as mentioned above to afford the sulfinylcalix[3]pyridine complex, [Rh{$Py_3(SO)_3$}(nbd)](BPh_4) (**6b**) (234 mg, 68%) (Found: C, 62.14; H, 4.10; N, 4.70. $C_{46}H_{37}N_3BO_3RhS_3$ requires C, 62.10; H, 4.19; N, 4.72%); δ_H(300 MHz, CD_2Cl_2, TMS) 8.21 (9H, AB_2 multiplet, pyridyl), 7.26 (8H, m, *o*-phenyl), 6.97 (8H, t, $^3J_{H-H}$ = 7.5 Hz, *m*-phenyl), 6.81 (4H, t, $^3J_{H-H}$ = 7.2 Hz, *p*-phenyl), 3.93 (4H, dd, J = 2.1 and 5.0 Hz, –C*H*=), 3.79 (2H, m, –C*H*–), 1.39 (2H, t, $^3J_{H-H}$ = 1.6 Hz, H-bridge-head); ESI-MS m/z = 570 ([M − BPh_4]$^+$). Prolonged reaction time (3 weeks) gave the tetraoxygenated complex, [Rh{$Py_3(SO)_2(SO_2)$}(nbd)](BPh_4) (**7b**), as a mixture with **6b**. δ_H(300 MHz, CD_2Cl_2, TMS) 8.53 (2H, d, J = 8.1 Hz, pyridyl), 8.38 (2H, d, J = 7.7 Hz, pyridyl), 8.25 (2H, d, J = 7.9 Hz, pyridyl), 8.05 (3H, AB_2 multiplet, pyridyl), 7.26 (8H, m, *o*-phenyl), 6.95 (8H, t, $^3J_{H-H}$ = 7.4 Hz, *m*-phenyl), 6.79 (4H, t, $^3J_{H-H}$ = 7.2 Hz, *p*-phenyl), 4.04 (4H, dd, J = 2.0 and 5.0 Hz, –C*H*=), 3.72 (2H, br, –C*H*–), 1.42 (2H, br, H-bridge-head); ESI-MS m/z = 586 ([M − BPh_4]$^+$). Shorter reaction time (2 h) afforded a mixture of monooxygenated [Rh{$Py_3S_2(SO)$}(nbd)](BPh_4) (**4b**) and dioxygenated [Rh{$Py_3S(SO)_2$}(nbd)](BPh_4) (**5b**) complexes confirmed by ESI mass spectrometry and X-ray diffraction study.

Oxidation of [Rh(Py_3S_3)(cod)]Cl by H_2O_2. To a solution of **1a** (115 mg, 0.200 mmol) in 20 mL of H_2O, 1 mL of 30% H_2O_2 aq was added and the mixture was stirred for 24 h. After a small amount of precipitate was filtered off, a solution of $NaBPh_4$ 137 mg, 0.400 mmol) in 5 mL of H_2O was added to the filtrate to give a yellow precipitate. After standing for 1 h, the precipitate was collected by filtration, washed with methanol and recrystallised from CH_2Cl_2 solution by addition of methanol. The precipitate contained the BPh_4 salt of the starting material and a small amount of the cod oxygenated complex, **8b** (102 mg). Prolonged reaction times caused decomposition of the complexes. Pure **8b** for X-ray crystallography was obtained by repeated recrystallisation by slow diffusion of methanol to a CH_2Cl_2 solution. δ_H(600 MHz, CD_2Cl_2, TMS) Assignment of the NMR signals follows the numbering scheme in Fig. 10. 7.55 (9H, br, pyridyl), 7.31 (8H, m, *o*-phenyl), 6.98 (8H, t, $^3J_{H-H}$ = 6.4 Hz, *m*-phenyl), 6.82 (4H, t, $^3J_{H-H}$ = 7.1 Hz, *p*-phenyl), 5.95 (1H, q, J = 5.3 Hz, H_7), 5.77 (1H, q, J = 5.3 Hz, H_5), 4.80 (1H, d, J = 6.4 Hz, H_1), 4.39 (1H, t, J = 8.0 Hz, H_6), 3.15 (1H, d, J = 0.8 Hz, H_2), 1.89 (1H, m, H_9), 1.84 (1H, m, H_4), 1.82 (1H, m, H_{11}), 1.35 (1H, dt, J = 14.7, 4.7 Hz, H_3), 1.10 (1H, m, H_8), 1.06 (1H, m, H_{10}); δ_C(150 MHz, CD_2Cl_2, TMS) 164.4 (q, J_{C-B} = 49.5 Hz, *i*-phenyl), 156.5 (s, 2,6-pyridyl), 139.8 (s, 4-pyridyl), 136.3 (s, o-phenyl), 129.2 (s, 3,5-pyridyl), 126.0 (s, *m*-phenyl), 122.1 (s, *p*-phenyl), 96.6 (d, $^1J_{C-Rh}$ = 6.2 Hz, C_5), 87.1 (d, $^2J_{C-Rh}$ = 0.8 Hz, C_2), 79.5 (d, $^1J_{C-Rh}$ = 11.8 Hz, C_6), 73.5 (d,

Table 2 Crystallographic data and structure refinement details for **1b**, **2b**, **3b**, the mixed crystal of **4b/5b**, **6b** and **8b**

	1b	**2b**	**3b**	**4b/5b**	**6b**	**8b**
Formula	$C_{47}H_{41}BN_3RhS_3$	$C_{46}H_{37}BN_3RhS_3$	$C_{47}H_{41}BN_3O_3RhS_3$	$C_{46}H_{37}BN_3O_{1.73}RhS_3$	$C_{46}H_{37}BN_3O_3RhS_3$	$C_{47}H_{41}BN_3ORhS_3$
M_r	857.76	841.71	905.75	869.39	889.71	873.76
T/K	193(1)	193(1)	193(1)	193(1)	193(1)	193(1)
Radiation used, λ/Å	Mo-Kα, 0.7107	Mo-Kα, 0.7107	Mo-Kα, 0.7107	Mo-Kα, 0.7107	Mo-Kα, 0.7107	Mo-Kα, 0.7107
Crystal description	Orange, prism	Orange, prism	Yellow, plate	Yellow, prism	Yellow, prism	Orange, prism
Crystal size/mm	0.10 × 0.25 × 0.25	0.15 × 0.15 × 0.25	0.05 × 0.25 × 0.30	0.07 × 0.10 × 0.10	0.10 × 0.20 × 0.30	0.10 × 0.15 × 0.25
Crystal system	Monoclinic	Monoclinic	Monoclinic	Monoclinic	Monoclinic	Monoclinic
Space group	$P2_1/c$	$P2_1/n$	$P2_1/n$	$P\bar{1}$	$P2_1/n$	$P2_1$
a/Å	15.254(2)	9.5391(9)	14.101(1)	10.170(2)	14.274(2)	9.569(1)
b/Å	14.629(2)	20.336(2)	17.712(2)	11.684(3)	16.733(2)	32.467(5)
c/Å	17.330(3)	19.527(2)	16.082(2)	17.496(4)	16.190(2)	12.727(2)
α/°	90	90	90	104.214(4)	90	90
β/°	91.691(3)	93.433(2)	93.231(2)	104.410(4)	95.333(3)	96.504(6)
γ/°	90	90	90	94.148(3)	90	90
V/Å	3865(1)	3781.3(6)	4010.0(7)	1932.0(7)	3850.1(8)	3928.6(10)
Z	4	4	4	2	4	4
F(000)	1768.00	1728.00	1864.00	891.68	1824.00	1800.00
ρ_{calcd}/g cm^{-3}	1.474	1.478	1.500	1.494	1.535	1.477
μ/mm^{-1}	0.642	0.655	0.629	0.647	0.654	0.635
Total reflections	37799	38438	40725	19003	38044	28849
Unique reflections	8683	8582	9103	8337	8726	15032
R(int)	0.064	0.032	0.035	0.045	0.045	0.064
Data/restrains/parameters	8683/0/660	8582/0/635	9103/0/687	8337/0/654	8726/0/662	15032/0/1009
$R1$ [$I > 2\sigma(I)$], $wR2$ (all data)	0.0672, 0.0874	0.0432, 0.0909	0.0396, 0.0828	0.0494, 0.0760	0.0385, 0.0640	0.0760, 0.1853
Goodness of fit on F^2	1.187	1.108	1.113	0.999	1.030	1.068
Max./min. e$^-$ densities/e Å^{-3}	0.34/−0.42	1.21/−0.57	0.38/−0.42	0.50/−0.59	0.69/−0.51	0.71/−0.95
Min./max. T factors	0.868/0.941	0.850/0.913	0.843/0.959	0.919/0.939	0.867/0.921	0.899/0.948

$^1J_{C-Rh} = 12.9$ Hz, C_4), 52.6 (d, $^1J_{C-Rh} = 21.4$ Hz, C_1), 39.9 (s, C_8), 35.6 (s, C_3), 24.6 (s, C_7); ESI-MS $m/z = 554$ ($[M - BPh_4]^+$).

Counter anion replacement of S-oxygenated complexes from BPh_4 to Cl

Into an acetone solution of a corresponding BPh_4 salt of each S-oxygenated complex, a small amount of conc. HCl aq was added. After stirring for 1 h, the solvent was removed under reduced pressure to give a yellow residue. The residue was re-dissolved in a small amount of methanol and any insoluble solid was filtered off. Addition of diethyl ether to the filtrate afforded a yellow precipitate which was collected by filtration (Yield 60–80%).

Crystal growth and X-ray crystallography

Single crystals of **1b, 2b** and **8b** were obtained by diffusion of methanol into a solution of the complex in $CHCl_3$ or CH_2Cl_2, at room temperature. Single crystals of **3b** were obtained by diffusion of cyclohexane into a solution of the complex in CH_2Cl_2. Mixed crystals of **4b/5b** were obtained from a solution of the mixture of the complexes in CH_2Cl_2 and methanol by slow evaporation of the solvents. Single crystals of **6b** were obtained by slow diffusion of a $NaBPh_4$ solution in methanol into a methanol solution of a Cl salt of the complex. Each single crystal was mounted on a glass fibre. Diffraction data were collected on an AFC7/CCD Mercury diffractometer using a rotation method with 0.3 for **8b** and 0.5 frame width for the others and with 5 s for **1b** and **6b** and 10 s for **2b, 3b, 4b/5b** and **8b** exposure times per frame. The data were integrated, scaled, sorted and averaged using CrystalClear[9] software. Absorption corrections were applied using Coppens numerical method. The structures were solved using SIR97[10] and refined with SHELXL97[11] using teXsan[12] as a graphical interface. Crystallographic data are summarised in Table 2. All non-hydrogen atoms were refined anisotropically. All hydrogen atoms except for those in **8b** were found in difference Fourier maps and refined isotropically. Hydrogen atoms in **8b** were located at calculated positions and refined as riding models. The site occupancy of the disordered oxygen atom in the mixed crystal **4b/5b** was refined.

CCDC reference numbers 237066, 237067 and 266664–266667.

See http://www.rsc.org/suppdata/dt/b5/b503924j/ for crystallographic data in CIF or other electronic format.

References

1 A. N. Vedernikov and K. G. Caulton, *Chem. Commun.*, 2003, 358.
2 (*a*) V. Král, P. A. Gale, P. Anzenbacher, Jr., K. Jursíková, V. Lynch and J. L. Sessler, *Chem. Commun.*, 1998, 9; (*b*) R. Crescenzi, E. Solari, C. Floriani, N. Re, A. Chiesi-Villa and C. Rizzoli, *Organometallics*, 1999, **18**, 606.
3 (*a*) R. Tanaka, T. Yano, T. Nishioka, K. Nakajo, B. K. Breedlove, K. Kimura, I. Kinoshita and K. Isobe, *Chem. Commun.*, 2002, 1686; (*b*) I. Kinoshita, A. Hamazawa, T. Nishioka, H. Adachi, H. Suzuki, Y. Miyazaki, A. Tstuboyama, S. Okada and M. Hoshino, *Chem. Phys. Lett.*, 2003, **371**, 451; (*c*) I. Kinoshita, L. J. Wright, S. Kubo, K. Kimura, A. Sakata, T. Yano, R. Miyamoto, T. Nishioka and K. Isobe, *Dalton Trans.*, 2003, 1993.
4 (*a*) L. Fabbrizzi and D. M. Proserpio, *J. Chem. Soc., Dalton Trans.*, 1989, 229; (*b*) K. Wieghardt, W. Schmidt, W. Herrman and H.-J. Küppers, *Inorg. Chem.*, 1983, **22**, 2953; (*c*) A. McAuley, P. R. Norman and O. Olubuyide, *Inorg. Chem.*, 1984, **23**, 1938; (*d*) A. McAuley, P. R. Norman and O. Olubuyide, *J. Chem. Soc., Dalton Trans.*, 1984, 1501.
5 (*a*) B. de Bruin, M. J. Boerakker, J. J. J. M. Donnors, B. E. C. Christiaans, P. P. J. Schlebos, R. de Gelder, J. M. M. Smits, A. L. Spek and A. W. Gal, *Angew. Chem., Int. Ed. Engl.*, 1997, **36**, 2064; (*b*) B. de Bruin, J. A. Brands, J. J. J. M. Donnors, M. P. J. Donners, R. de Gelder, J. M. M. Smits, A. W. Gal and A. L. Spek, *Chem. Eur. J.*, 1999, **5**, 2921.
6 N. Morohashi, H. Katagiri, N. Iki, Y. Yamane, C. Kabuto, T. Hattori and S. Miyano, *J. Org. Chem.*, 2003, **68**, 2324.
7 (*a*) K. R. Reistad, P. Groth, R. Lie and K. Undheim, *J. Chem. Soc., Chem. Commun.*, 1972, 1059; (*b*) P. Groth, *Acta Chem. Scand.*, 1973, **27**, 5.
8 *Crystal Clear*, Rigaku Corp., Woodlands, TX, 1999.
9 A. Altomare, M. C. Burla, M. Camalli, G. Cascarano, C. Giacovazzo, A. Guagliardi, A. G. G. Moliterni, G. Polidori and R. Spagna, *J. Appl. Crystallogr.*, 1999, **32**, 115.
10 G. M. Sheldrick, *SHELX-97, Program for Crystal Structure Refinement*, University of Göttingen, Göttingen, Germany, 1997.
11 *teXsan, Crystal Structure Analysis Package*, Molecular Structure Corp., Houston, TX, 1985 and 1992.
12 T. C. Flood, M. Iimura, J. M. Perotti, A. L. Reingold and T. E. Concolino, *Chem. Commun.*, 2000, 1681.